Atmospheric turbulence profiling with the Laser Communication Relay Demonstration experiment and RINGSS at Table Mountain Facility, California

Marcus Birch
Advanced Instrumentation Technology Centre, Research School of Astronomy and Astrophysics, Australian National University, Canberra, ACT 2611, Australia
Jet Propulsion Laboratory, California Institute of Technology, Pasadena, CA, USA 91109

Sabino Piazzolla, Preston Hooser, William Buehlman
Jet Propulsion Laboratory, California Institute of Technology, Pasadena, CA, USA 91109

Francis Bennet, Tony Travouillon
Advanced Instrumentation Technology Centre, Research School of Astronomy and Astrophysics, Australian National University, Canberra, ACT 2611, Australia

ABSTRACT

Adaptive optics has been used to mitigate the impact of atmospheric turbulence on laser propagation through the atmosphere, and to restore diffraction limited imaging to large optical apertures. Understanding the turbulence characteristics of a particular site enables an optimised adaptive optics design. We present a novel turbulence profiling technique: a Ring Image Next Generation Scintillation Sensor (RINGSS), adapted for infrared wavelengths can measure both integrated turbulence and the profile. We report on results from a deployed system at the NASA/Jet Propulsion Laboratory's Table Mountain Facility. The downlink from the Laser Communication Relay Demonstration (LCRD) geostationary spacecraft terminal as a reference for atmospheric turbulence profiling. LCRD beam allows for high signal-to-noise at all times of day and night through the same atmospheric channel as the optical ground station conducting the link. The RINGSS measurement technique is robust even in strong daytime turbulence with comparison to other instruments. This demonstrates the utility of RINGSS for turbulence profiling could be effectively used to design effective adaptive optics for 24 hour operations.

1. INTRODUCTION

Optical telescopes play a crucial role in space domain awareness (SDA), providing valuable tools for imaging and tracking satellites, detecting space debris, and conducting satellite laser ranging (SLR). High-resolution imaging of satellites from ground-based optical systems provides detailed information on satellite structures, orientation, and activity. Satellite laser ranging delivers precise measurements of satellite orbits with millimeter accuracy, aiding collision avoidance and orbital determination with high precision. However, one of the significant challenges faced by ground-based optical telescopes is the impact of atmospheric turbulence. This turbulence, caused by temperature fluctuations and variations in air density, distorts the wavefront of light, leading to degraded image quality and reduced accuracy in optical measurements including laser propagation. To mitigate these effects, techniques like adaptive optics are employed to correct for real-time atmospheric distortions, significantly enhancing the performance of optical systems in SDA applications.

Laser propagation activities such as satellite laser ranging, and high bit-rate or quantum free-space optical communication (FSOC) technologies [8, 6] suffer more from atmospheric turbulence than imaging techniques because the distortions are encountered as the first element of propagation after the optical telescope aperture. These disturbances then continue to propagate to the target, resulting in larger diffraction than from a diffraction limited optical system. Imaging systems encounter turbulence last in the propagation, with the greatest portion of propagation occurring in space or thin atmosphere without impact on the optical signal.

Lasers propagating through atmospheric turbulence not only suffer from greater impacts of turbulence due to diffraction, but the coherent nature of the laser light results in both phase and intensity fluctuations on both up- and down-link laser beams. Depending on the application, these fluctuations may have a significant impact on the laser purpose, such as communication, time transfer, or other techniques requiring precise phase measurements.

It is therefore vital to fully understand the characteristics of atmospheric turbulence at a particular site to develop an optical system that can improve compensation methods, such as adaptive optics. Site testing data can be used to inform where to place optical telescopes for a performance metric, and potentially allow short-term forecasting of turbulent conditions to assist in optimising control systems [5], and can be combined with cloud cover analysis to provide a location-based prediction of overall site performance. SDA techniques such as optical imaging of satellites with adaptive optics, enhanced SLR, and improvements to laser propagation will benefit greatly from understanding the optical characteristics of a proposed site.

2. ATMOSPHERIC SITE TESTING

Atmospheric turbulence and site testing are well studied fields with campaigns frequently used to select the best astronomical observing sites. Turbulence itself is not straight-forward to measure and is typically done by observing celestial objects and estimating the integral of turbulence through the entire atmospheric column. The coherence length of atmospheric turbulence is described by the Fried parameter, r_0, and is related to the optical turbulence profile (OTP) along an atmospheric column. Equation 1 provides the definition for r_0 where C_n^2 is the coefficient of the structure function of refractive index. C_n^2 describes the turbulence strength for an infinitesimal layer with units of $m^{-2/3}$ and C_n^2 as a function of altitude is effectively the OTP.

$$r_0 = \left[16.7\lambda^{-2}\int C_n^2(z)dz\right]^{-3/5} \tag{1}$$

Differential Image Motion Monitors (DIMMs) are the most common instruments for measuring integrated turbulence [10]. However, measuring the integrated column of turbulence does not convey the complete story of the impact of turbulence on laser propagation. The effect of atmospheric turbulence on phase error for a received or transmitted laser beam is intricately related to the propagation of that beam through the column of continuously varying turbulence. The phase errors imprinted on a laser beam propagate and vary between amplitude and phase distortions while the beam remains coherent. Measuring the OTP rather than integrated turbulence can be beneficial for tuning adaptive optics systems, or potentially driving short-term forecasting of conditions to improve network resiliency [6, 7]. A means of turbulence profiling specific to FSOC is presented here [1]. FSOC turbulence profiling uses a satellite laser terminal downlink as point source above the atmospheric column rather than stars which are generally used. A satellite in Geostationary orbit (GEO) appears nearly stationary with respect to ground observer, making them an ideal source for FSOC turbulence profiling. An FSOC downlink, as opposed to a star, has the primary advantage of a narrow spectrum laser source rather than broadband stellar radiation. This means a filter can be used to reject background noise and observations are possible at all times of day, and even to shallow solar separation angles. However, this technique does require the turbulence monitor to be within the beam footprint of a downlink, i.e. in proximity to the optical ground station conducting the link. This limits the application to an operational support role, rather than for testing prospective ground station sites. FSOC turbulence profiling is demonstrated here by installing RINGSS instrument at NASA/JPL's Table Mountain Facility (TMF), California and observing the downlink from the *Laser Communication Relay Demonstration* (LCRD) GEO experiment [9]. LCRD is a laser relay terminal with two optical heads that is launched in 2021 and communications around 1550 nm [3]. This experiment between RINGSS and LCRD was done while the the OGS-1/Optical Communications Telescope Laboratory (OCTL) was conducting bi-directional links with LCRD.

3. RINGSS DESCRIPTION

Figure 1 shows RINGSS installed in its small sliding-roof enclosure and indicates the proximity at TMF to OCTL. We use a 25 cm telescope with 320x256 InGaAs array with a C-band filter for LCRD(visible in Figure 1). RINGSS benefits from being built of entirely commercial off-the-shelf components and a reasonably small aperture. RINGSS is

Fig. 1: Table Mountain Facility, California with 10" RINGSS instrument located in the foreground. Inset: Position of RINGSS and OCTL.

an atmospheric turbulence monitoring instrument that measures the scintillation of defocused point sources to estimate the OTP. A defocused point-spread function appears as a ring with scintillation as angular variance which can be used for retrieving an estimating an angular frequency spectrum. This angular frequency spectra are subsequently related to weighting functions which parameterize modal dissipation with propagation. This is similar to instruments like the Multi-Aperture Scintillation Sensor (MASS), which all rely on solving some measured spectra against weighting functions computer prior [4]. Tokovinin (2021) provides a fundamental overview of the operational principle of RINGSS. There are a number of differences for observing a satellite downlink, e.g. the signal is monochromatic and infrared, and Birch et al. (2024) provides a review of these variations [1].

The LCRD downlink as imaged by RINGSS is a ring with of approximately 10 pixels and width of $2-3$ pixels. The radius describes defocus while the width is a function of focal length and optical alignment. Two second videos of the defocused ring are captured continually with the OTP averaged at each instance. The Fried parameter, r_0, and other parameters such as the isoplanatic angle are also estimated by integrating the OTP.RINGSS measures r_0 in two ways, i.e. through the integral of the OTP and through the radial motion of the ring image in a fashion related to the DIMM instrument. We refer to r_0 as computed from the integral of the OTP as $r_{0,\text{scint}}$ and the radial method as $r_{0,\text{sector}}$. All values of r_0 in this paper are scaled to 500 nm zenith-corrected, per convention.

4. RESULTS

LCRD was observed with RINGSS over a number of days while bi-directional communication was occurring between LCRD and OCTL. Figure 2 shows the two methods for measuring r_0 are in good agreement over in this preliminary dataset. As mentioned prior, all r_0 values are for 500 nm and air-mass corrected to zenith. Observations of LCRD from TMF are at a zenith angle of approximately 40°. r_0 measurements are compared against a solar scintillometer and Polaris image motion monitor for daytime and nighttime respectively to determine the accuracy of this method. These comparison instruments are shown in Figure 3.

Figure 4 shows a time series of a sample of data, with both r_0 estimates from RINGSS and the comparison instruments. Good agreement is observed among all instruments, indicating that this method is valid, even in strong daytime turbulence. Note that these results rely on a very small sample of data, so assertions of validity are only preliminary.

Average day and night OTPs are shown in Figure 5., split into averages of daytime and nighttime. RINGSS measures turbulence in discrete layers of the atmosphere, hence why the y-axis of Figure 5 lists $C_n^2 dh$ rather than C_n^2 for the OTP. The width for each data point is from that height, z_i, to the following layer height, z_{i+1}. This OTP is has a vertical resolution given by eight data points, an improvement on other compact profilers such as the SHIMM but substantially lower than profilers such as SCIDAR [2]. The upper layer, denoted at 16 km, theoretically provides an estimate of

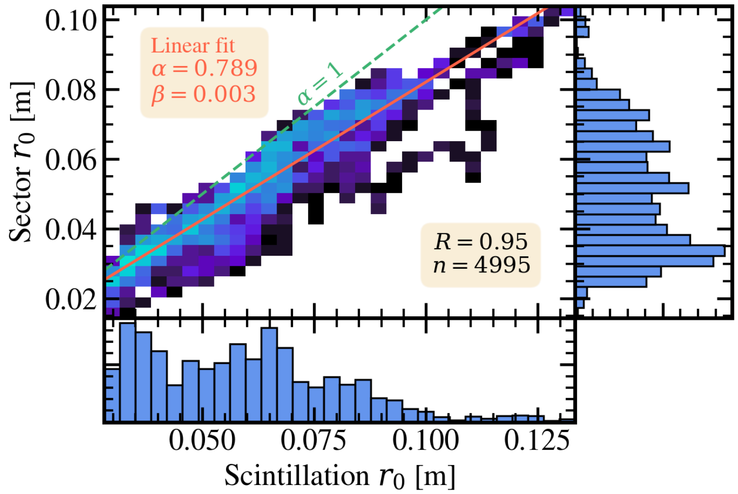

Fig. 2: Fried parameter, r_0, statistics from entire preliminary dataset of RINGSS at TMF observing the LCRD downlink. Scintillation r_0 is the OTP integral and sector r_0 is the radial motion of the ring.

Fig. 3: Polaris image motion monitor and solar scintillometer at TMF. Polaris monitor is located on the roof of OCTL and at a height above RINGSS.

turbulence strength from that height to the top of the atmosphere.

The OTPs show the typical diurnal evolution for atmospheric turbulence, i.e. stronger turbulence near the surface in the daytime. The daytime profile has a feature of very weak turbulence from 4 km to 8 km which is a possible indication of scintillation saturation [9]. This does show the limitation of scintillation sensors in strong turbulence but more work is required to investigate this feature, as it could also be a physical property.

This highlights the benefit of a profiler, being able to distinguish the characteristic turbulence height. Furthermore, a number of integrated parameters such as the coherence time or isoplanatic angle require an OTP for estimation. We compute coherence times of 1.5 ms to 3.5 ms and isoplanatic angles of 1.2 to 2.5 arcseconds.

5. CONCLUSION

Observations and measurements from optical telescopes provide a range of high-precision data used for SDA, but are degraded by optical turbulence. While techniques exist to mitigate the impacts of optical turbulence such as adaptive optics, such systems must be built for purpose to match the site turbulence conditions expected. Turbulence can be measured as an integrated metric or with a turbulence profiler. We present the application of a compact turbulence profiler and have successfully measured the profile of atmospheric turbulence using the downlink from a laser com-

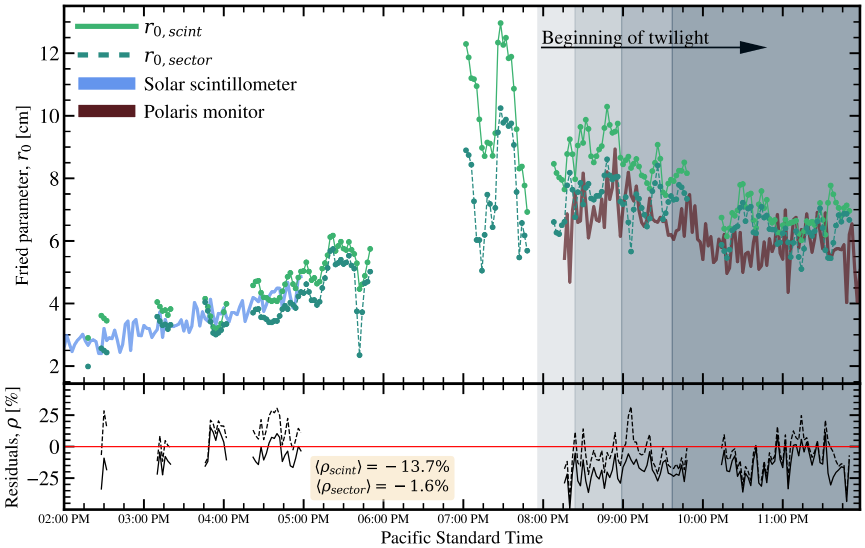

Fig. 4: Fried parameter, r_0, time series from various turbulence monitors at TMF, including two separate estimates from RINGSS. Data is from the 23rd of May, 2023. Relative residuals from comparing RINGSS against the Polaris monitor and solar scintillometer are shown in the inset.

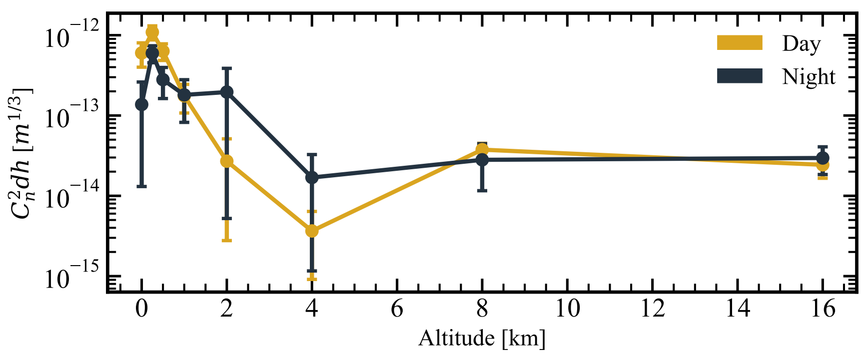

Fig. 5: Optical turbulence profiles estimated by RINGSS. Diurnal evolution is shown with statistical bins into daytime and nighttime turbulence. Atmospheric turbulence strength with altitude is given by the discrete layers of $C_n^2 dh$ and units $m^{1/3}$.

munication satellite to demonstrate the capability for 24 hour monitoring of a turbulence profile. The measurements were robust in strong turbulence and confirm this concept's efficacy at infrared wavelengths under both day and night conditions. This concept could also be extended to horizontal turbulence measurements in a similar manner to boundary layer scintillometers to aid in understanding the impacts on horizontal laser propagation. The RINGSS system will undergo further cross-instrument comparisons with other turbulence monitors and profilers around the world. The application of this technique will enable better site selection for future optical SDA telescopes, and better design choices when upgrading existing systesm with adaptive optics.

ACKNOWLEDGEMENTS

The research was carried out at the Jet Propulsion Laboratory, California Institute of Technology, under a contract with the National Aeronautics and Space Administration. The authors would like to thank the LCRD and OCTL operational teams.

More details on this research can be found in [1], which is a more thorough journal paper on this research.

[1] Marcus Birch, Sabino Piazzolla, Preston Hooser, Francis Bennet, Tony Travouillon, and William Buehlman. Optical turbulence profiling at the table mountain facility with the laser communication relay demonstration geo downlink. *Optics Express*, 32(12):21962–21976, 2024.

[2] R Griffiths, L Bardou, T Butterley, J Osborn, R Wilson, E Bustos, A Tokovinin, M Le Louarn, and A Otarola. A comparison of next-generation turbulence profiling instruments at Paranal. *Monthly Notices of the Royal Astronomical Society*, page stae434, 2024.

[3] David J Israel, Bernard L Edwards, Richard L Butler, John D Moores, Sabino Piazzolla, Nic du Toit, and Lena Braatz. Early results from NASA's laser communications relay demonstration (LCRD) experiment program. In *Free-Space Laser Communications XXXV*, volume 12413, pages 10–24. SPIE, 2023.

[4] Victor Kornilov, Andrei A Tokovinin, Olga Vozyakova, Andrei Zaitsev, Nicolai Shatsky, Serguei F Potanin, and Marc S Sarazin. MASS: a monitor of the vertical turbulence distribution. In *Adaptive Optical System Technologies II*, volume 4839, pages 837–845. SPIE, 2003.

[5] James Osborn and Marc Sarazin. Atmospheric turbulence forecasting with a general circulation model for Cerro Paranal. *Monthly Notices of the Royal Astronomical Society*, 480(1):1278–1299, 2018.

[6] Sabino Piazzolla, William T Roberts, Joseph Kovalik, Michael Peng, Vachik Garkanian, Christine Chen, William Buehlman, Mark Brewer, Gerardo Ortiz, Kittrin Matthews, et al. Ground station for terabyte infrared delivery (TBIRD). In *Free-Space Laser Communications XXXV*, volume 12413, pages 280–295. SPIE, 2023.

[7] Florian Quatresooz, Ryan Griffiths, Lisa Bardou, Richard Wilson, James Osborn, Danielle Vanhoenacker-Janvier, and Claude Oestges. Continuous daytime and nighttime forecast of atmospheric optical turbulence from numerical weather prediction models. *Optics Express*, 31(21):33850–33872, 2023.

[8] Curt M Schieler, Kathleen M Riesing, Bryan C Bilyeu, Jesse S Chang, Ajay S Garg, Noah J Gilbert, Andrew J Horvath, Robert S Reeve, Bryan S Robinson, Jade P Wang, et al. On-orbit demonstration of 200-Gbps laser communication downlink from the TBIRD CubeSat. In *Free-Space Laser Communications XXXV*, volume 12413, page 1241302. SPIE, 2023.

[9] Andrei Tokovinin. Measurement of turbulence profile from defocused ring images. *Monthly Notices of the Royal Astronomical Society*, 502(1):794–808, 2021.

[10] Andrei Tokovinin. The Elusive Nature of "Seeing". *Atmosphere*, 14(11):1694, 2023.